In situ Detection of Cracks During Electroplating Processes By Acoustic Emission

by Tsutomu Morikawa* & Kanji Ono

Electroplating processes have long been known to generate acoustic emission (AE) signals. These originate from crack formation and hydrogen bubble evolution-and-collapse during electroplating. However, few studies have been done recently, although AE is now a standard technique in monitoring the adhesion of plated/coated films in conjunction with scratching. We recorded AE signals during the electroplating of copper, nickel and chromium on copper and stainless steel sheets, by varying the conditions of electroplating (solution composition, pH level, bath temperature and current density). AE waveforms exhibit distinct plate-wave characteristics, with cracks giving strong extensional modes and hydrogen bubbles having mostly flexural waves. Waveform- or frequency-based discrimination can be easily performed to separate the two signal types. Signal amplitude can also be used to discriminate weak AE signals from the bubbles. Applications to *in situ* monitoring of electroplating processes are discussed.

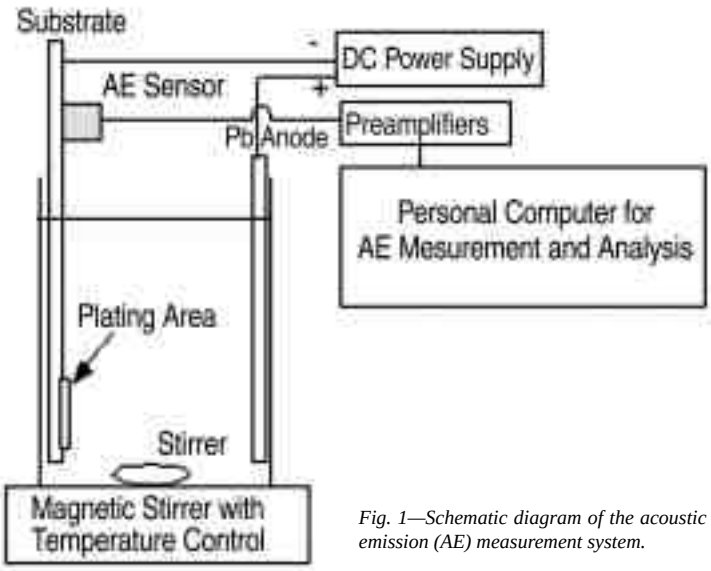

Fig. 1—Schematic diagram of the acoustic emission (AE) measurement system.

Nuts & Bolts: What This Paper Means to You

Crack formation and hydrogen bubble evolution-and-collapse during plating have been known to generate acoustic emission (AE) signals. AE is commonly used in monitoring scratch adhesion of plated films, but studies of the plating process itself have been limited. Here, the authors explored the characteristics of AE signals during copper, nickel and chromium plating on copper and stainless steel sheets. There is potential here for in-tank monitoring of electroplating processes. Imagine controlling chromium crack patterns or hydrogen embrittlement this way.

It is important to evaluate and control accurately the conditions of surface cracks in plated coatings, when the functionality of plated surfaces depends on these cracks. Some hard coatings and films exhibit microcracks as a result of the plating processes themselves. Chromium plating is the best known example and surface crack densities of tens to hundreds per lineal cm are typically observed. These cracks are closely related to the hardness and ductility of the plated coatings and affect the corrosion and wear resistance of the plated surfaces. Cracks in the coatings can seriously reduce the desired corrosion and abrasion resistance. Conversely, these cracks can also have beneficial effects, as in "microcracked chromium plating," in which numerous surface cracks disperse corrosion current and improve the corrosion resistance, and in "porous chromium plating" that retains lubricant in the surface cracks and enhances its wear resistance.

We have limited means of non-destructively evaluating plated coatings. High internal stresses are typically present in the plated coatings with cracks, as the stresses are believed to be the cause of cracking. The internal stress in a coating is measured by using spiral contractometers and glancing angle x-ray diffractometers. However, quantitative treatment becomes difficult once cracks are formed. Consequently, the coatings are evaluated only indirectly by microscopic measurement of crack count on the surface and cross-section of the coatings, by qualitative observation of crack morphology and by monitoring the degree of corrosion in various corrosion tests.

In this study, we have examined the applicability of acoustic emission (AE) analysis in evaluating cracking in coatings during electroplating. Takano and Ono[1] reported in 1974 that AE can be detected during electroplating and electroless plating. Since their initial work, little has been reported, even though AE signal processing methods have been vastly improved. Thin structures are typically used for plating substrates. Under such a condition, AE signals propagate as Lamb waves and this aspect needs to be considered as well.

**Corresponding Author:*
Tsutomu Morikawa
Technology Research Institute of Osaka Prefecture
2-7-1 Ayumino
Izumi, Osaka, 594-1157 Japan
E-mail: morikawa@tri.pref.osaka.jp

Experimental

In the first phase of this study, we selected chromium plating to establish measurement conditions and evaluate the effectiveness of the AE approach. The chromium plating solution composition was 250 g/L CrO_3 and 2.5 g/L H_2SO_4. The solution temperature was varied from 30 to 60°C (86 to 140°F), and the cathode current density was varied from 20 to 70 A/dm^2 (186 to 650 A/ft^2). A 200-mL solution volume was used in a 300-mL beaker. The substrates used were copper sheets (150 x 25 x 0.2 mm; approx. 6 x 1 x 0.008 in.) and the anode was a lead plate. The actual plating area was 20 x 20 mm (0.79 x 0.79 in.), or 4 cm^2 (0.62 in^2.) at 5 mm (0.2 in.) from the bottom end. The immersed region outside the plating area was covered with insulating tape. Before plating, the substrate was electrocleaned for 1 min in an alkaline solution at 50 to 60°C (122 to 140°F) (20 g/L NaOH; 20 g/L $NaCO_3$). Figure 1 shows a schematic diagram of the plating experiment.

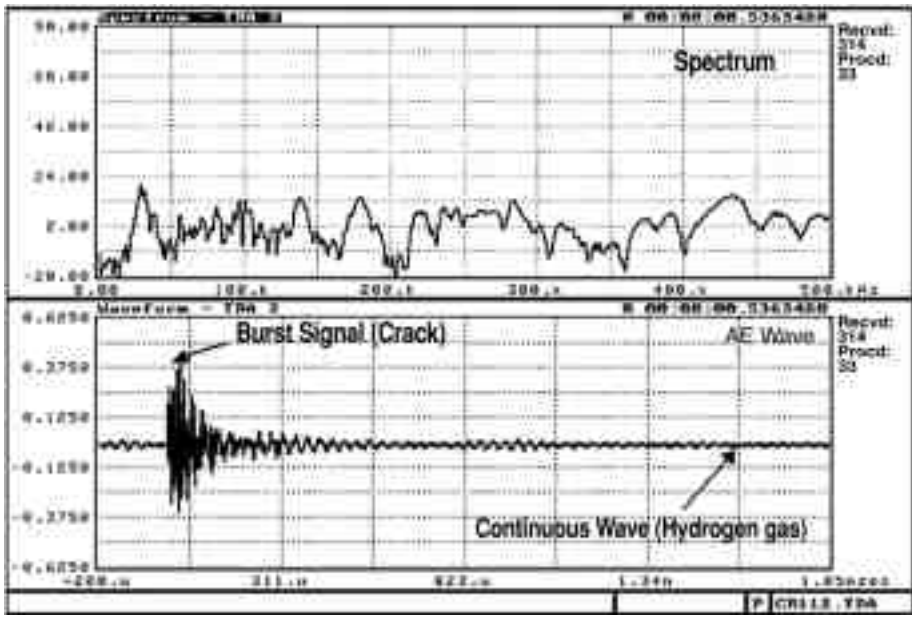

Fig. 2—Typical AE signals observed during chromium plating.

After the chromium plating work, other plating systems evaluated with AE measurements. The systems studied in this second phase were copper, nickel, Ni-B and Ni-P. The Ni-B plating solution consisted of 100 g/L $NiSO_4.6H_2O$, 30 g/L $NiCl_2.6H_2O$, 30 g/L H_3BO_3, 10 g/L sodium citrate and 1 g/L DMAB . The plating conditions were pH 4.5, a solution temperature of 40°C (104°F) and a current density of 3.0 A/dm^2 (27.9 A/ft^2). For Ni-P plating, the solution contained 100 g/L $NiSO_4.6H_2O$, 30 g/L $NiCl_2.6H_2O$, 30 g/L H_3BO_3, 145 g/L sodium citrate and 82 g/L H_3PO_3. Plating conditions were pH 3.5, 50°C (122°F) and 3.0 A/dm^2 (27.9 A/ft^2). Copper plating was done in a sulfuric acid solution.

The acoustic emission sensor used was a wide-band type[**] and was attached 120 mm (4.72 in.) from the bottom with resin couplant and electrical tape. A 60-dB pre-amplifier[***] and a processor board[****] installed on a 166-MHz PC were used for AE data acquisition with the waveform recording function activated. Various aspects of AE testing methods and instrumentation can be found in the literature.[2,3] The AE sensor used here is a piezoelectric type and detects mechanical waves propagating through the sample being plated. Because the thickness is much less than the wavelength, the waves are transmitted in plate-modes or as Lamb waves in contrast to the bulk waves typically used in ultrasonic non-destructive testing. The sensor generates electrical pulses corresponding to the mechanical waves. Such pulses are amplified and their occurrences (known as AE events), peak amplitude and duration, as well as the complete waveforms, are recorded as digital information. This information is used to evaluate the level and intensity of AE activities and to correlate the data to plating conditions and the quality of plating.

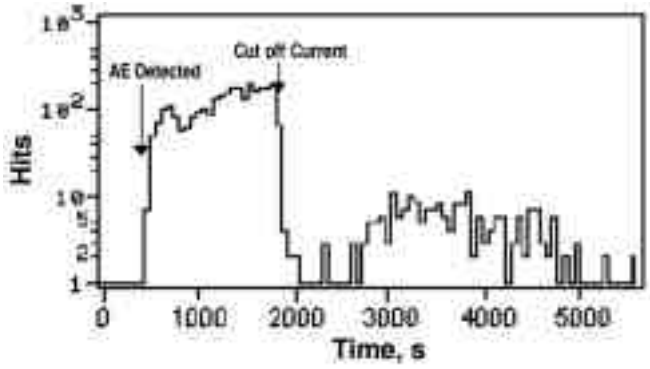

Fig. 3—Time dependence of AE hit rate (Solution temp. = 30°C / 86°F; CD = 20 A/dm^2/186 A/ft^2; AE Filter = 200-1200 kHz; 56 dB threshold.).

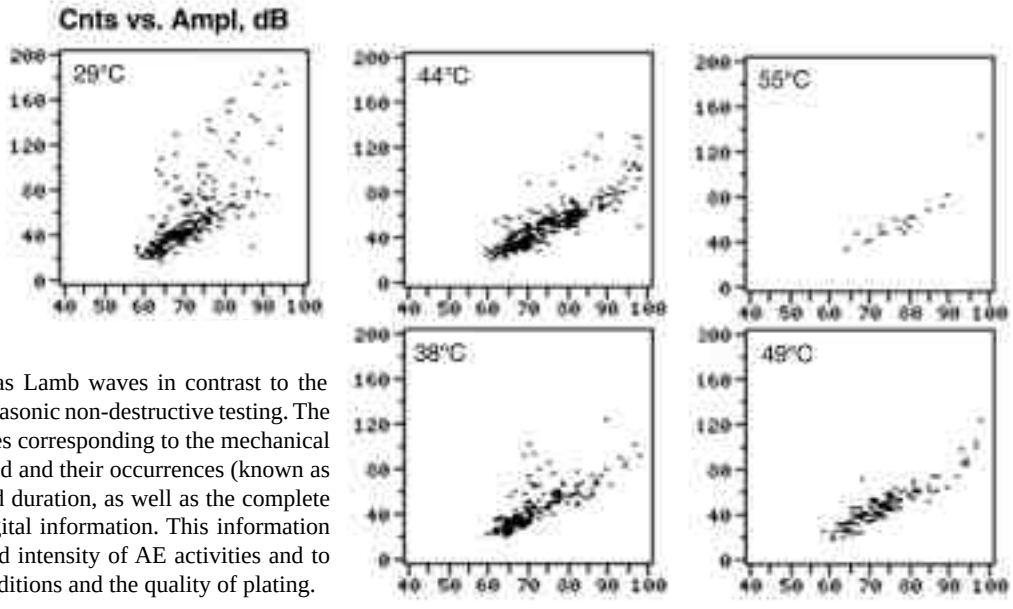

Fig. 4—AE hits vs. amplitude at five solution temperatures (CD = 20 A/dm^2/186 A/ft^2; AE Filter = 200-1200 kHz; 56 dB threshold.).

[**] *PAC-WD, Physical Acoustics Corporation, Princeton Junction, NJ.*
[***] *PAC-1220A, Physical Acoustics Corporation, Princeton Junction, NJ.*
[****] *PAC MISTRAS Board, Physical Acoustics Corporation, Princeton Junction, NJ.*

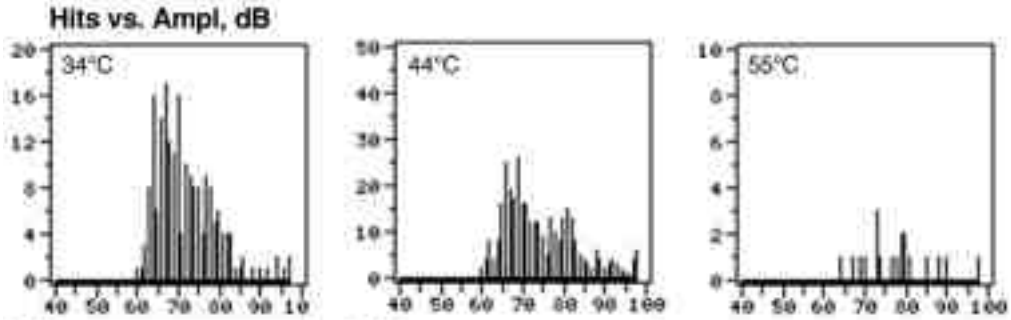

Fig. 5—AE amplitude distribution plots at five solution temperatures (CD = 20 A/dm²/186 A/ft²; AE Filter = 200-1200 kHz; 56 dB threshold).

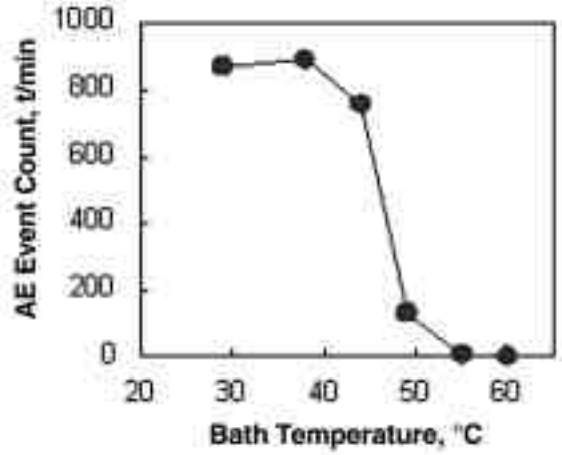

Fig. 6—Effect of bath temperature on AE event count during chromium plating (CD = 20 A/dm²/186 A/ft²; AE Filter = 200-1200 kHz; 56 dB threshold.).

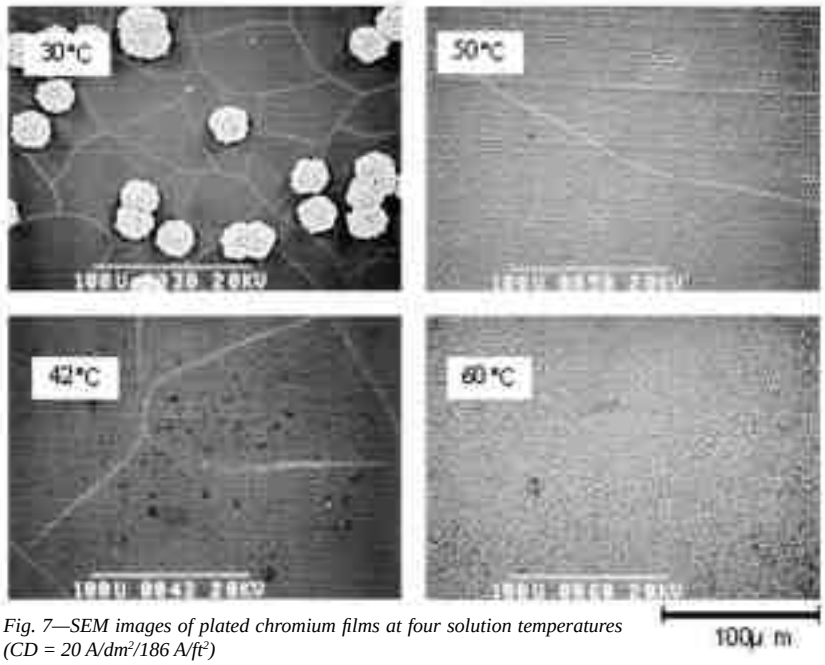

Fig. 7—SEM images of plated chromium films at four solution temperatures (CD = 20 A/dm²/186 A/ft²)

Results & Discussion

Hydrogen bubble discrimination

It is common to observe hydrogen bubbles on the substrate surface during plating. When such bubbles form and subsequently collapse, AE signals would be expected, as reported initially by Felson and Rettig[4] during corrosion of aluminum and by Takano and Ono[1] in their plating experiments. A preliminary experiment was conducted to find test parameters that eliminate counting these AE signals. This is necessary to reduce the number of signals requiring analysis and to simplify the processing for crack detection.

The typical signals observed during chromium plating are shown in Fig. 2, which shows two types of signals. One is a typical high-frequency burst-type with a sharp rise and slower decay, while the other is a low-frequency wave packet with lower amplitude. Approximately 99% of the latter signals can be discriminated by setting the filter range to 200-1200 kHz and the detection threshold at 56 dB. Low-frequency signals were also detected when only hydrogen bubbles were formed at the copper cathode in alkaline solution. This shows that hydrogen bubbles were the source of the low-frequency signals. In subsequent experiments, we used these settings to detect only crack-induced signals.

Acoustic emission behavior during chromium plating

The typical time dependence of the AE hit rate is shown in Fig. 3. The AE signals are detected after an incubation of 3 to 5 min and tend to saturate after 15 min. Acoustic emission was detected even after switching off the current and lasted for several hours. After an immediate drop in the AE hit rate with the current turned off, there was a 10 minute period of low AE activity. This AE behavior corresponds to general observations in chromium plating, where thin coatings of up to 0.3 to 0.5 µm (12 to 20 µ-in.) are free of cracks and plating reaches a steady state beyond a certain thickness (~1.5 µm; 5.9 µ-in. in the present example). Crack formation requires the build-up of internal tensile stresses and a minimum thickness, leading to acoustic emission. Cracks in chromium plating result from stresses induced by hydrogen absorbed during plating. Cracks corresponding to post-plating AE appear to come from atomic hydrogen diffusion toward crack nuclei and subsequent formation of hydrogen gas which later escapes through the cracks.

Plots of AE counts vs. amplitude and amplitude distribution at five different bath temperatures are shown in Figs. 4 and 5. A straight-line relation in AE counts vs. amplitude is noted, especially at high solution temperatures. This behavior resembles an exponential decay. However, higher counts are found at lower bath temperatures (<44°C; <111°F). This appears to arise from multiple events recorded as a single event, where hit rates are

higher at lower temperatures. This trend is shown in the plot of AE event count rates vs. temperature shown in Fig. 6. The AE rates diminished above solution temperatures of 60°C (140°F), while they reached a plateau below 36°C (97°F). This general trend agrees with the measured crack density, as shown in the SEM photos in Fig. 7. At 30°C (86°F), the crack density (cracks per lineal distance) was 250/cm (635/in.). At 42°C (108°F) it was 150/cm (381/in.), and at 50°C (122°F), 100/cm (254/in.). No cracks were found at 60°C (140°F).

The AE event rates however, were not proportional to the observed crack density. This was not unexpected, as we used a relatively high threshold. Normally, the numerous lower amplitude signals are not included in our measurement. This may also reflect the changes in the type of cracks generated, i.e., cracks tend to be shorter at lower temperatures. This trend is shown in the amplitude distribution. High amplitude events are relatively more numerous at higher temperatures, as shown in Fig. 5. From these observations, we find that crack counts decrease with increasing bath temperature, diminishing above 60°C (140°F). However, each crack produces stronger AE signals at higher temperatures. Note that a peak in Fig. 5 at about 65 dB is an artificial peak from using the 56 dB threshold. It is expected that more low-amplitude signals are present, but not included in the present measurement.

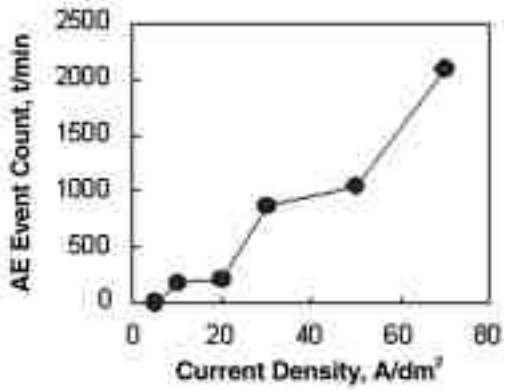

Fig. 8—Effect of current density on AE event count during chromium plating (Solution temperature = 44°C/111°F; AE Filter = 200-1200 kHz; 56 dB threshold.).

The effects of cathode current density on the nature of the cracks appear to be minimal. Figure 8 shows that AE event counts increase nearly linearly with current density. However, the shape of the amplitude distribution, shown in Fig. 9, changes little with the current density.

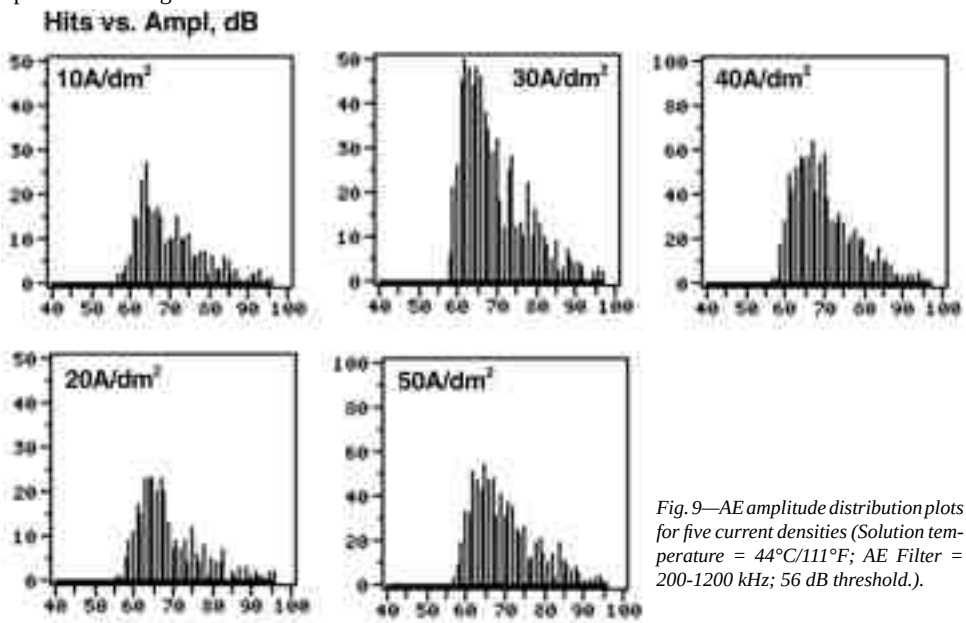

Fig. 9—AE amplitude distribution plots for five current densities (Solution temperature = 44°C/111°F; AE Filter = 200-1200 kHz; 56 dB threshold.).

Crack-free plating

In crack-free copper and nickel plating, no AE signal above the noise level was detected. This implies that the nuclei formation in the plating processes, crystallite junction and grain growth during plating produce no detectable acoustic emission.

Ni-B & Ni-P alloy plating

Nickel alloy plating of Ni-B and Ni-P is environment friendly and is expected to replace chromium plating. The presence of cracks in chromium deposits can contribute to loss of corrosion resistance. Thus, we examined AE behavior in these potential chromium replacements.

Figure 10 shows the SEM images of the Ni-B alloy film. The boron content was about 0.8 wt% and its hardness was 650 VHN. Figure 11 summarizes the AE characteristics in Ni-B plating. Acoustic emission was first observed after six minutes of plating and reached saturation after 50 min. The AE hit rates were comparable to those of chromium plating (cf. Fig. 4). The AE counts vs. amplitude plot shows trend like that found in chromium plating at comparable temperatures, but more high-amplitude signals were observed. This is also shown in the amplitude distribution plot, in which a peak at 87 dB is present. The crack density was about 100/cm.

Figure 12 shows the SEM images of the Ni-P alloy films. The phosphorus content was about 14 wt% and its hardness was 550 VHN. When compared to chromium or Ni-B plating, the acoustic emission signals for Ni-P were considerably reduced. Figure 13 shows one example. Acoustic emission was observed only after 35 min of plating and the hit rates were at most 10–20 counts/min. This rate was an order of magnitude smaller than for chromium or NiB (Figs. 3 and 10, respectively). Cracks in this plating were quite small in number and were observed only at higher current densities.

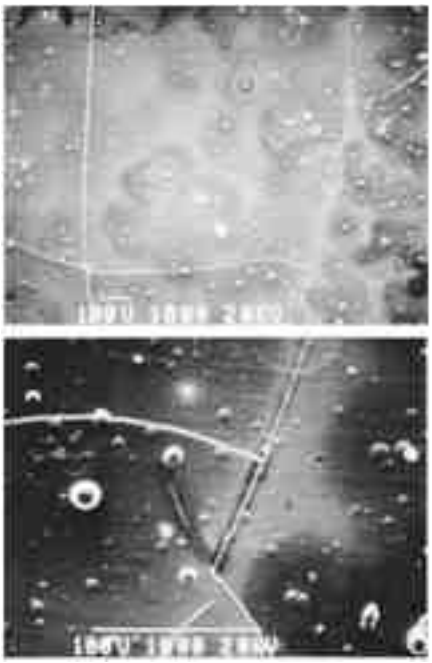

Fig. 10—SEM images of Ni-B alloy films (Solution temperature = 40°C/104°F; pH 4.5; CD = 3.0 A/dm² / 27.9 A/ft²).

Conclusions

We have evaluated acoustic emission (AE) behavior of electrodeposited chromium, crack-free copper and nickel and nickel alloys *in situ*. Acoustic emission signals originate from cracking as well as from hydrogen bubbles. The latter can be essentially eliminated from

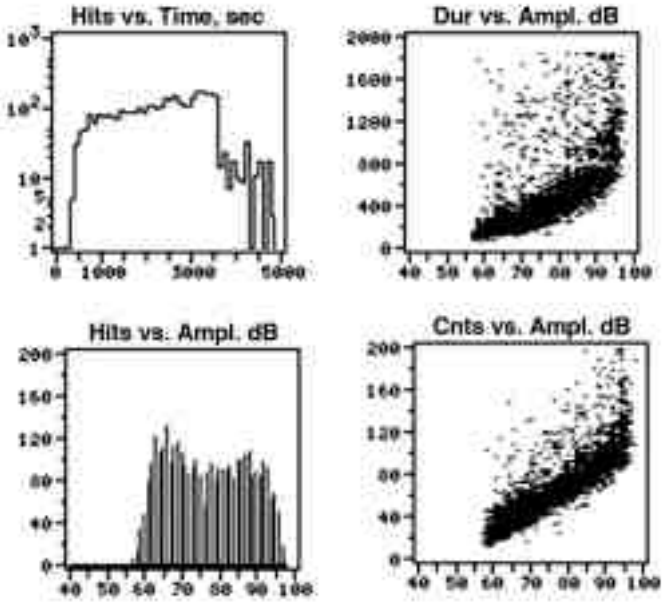

Fig. 11—Summary of AE characteristics in Ni-B plating (Solution temperature = 40°C/104°F; pH 4.5; CD = 3.0 A/dm²/27.9 A/ft²; AE Filter = 200-1200 kHz; 56 dB threshold.).

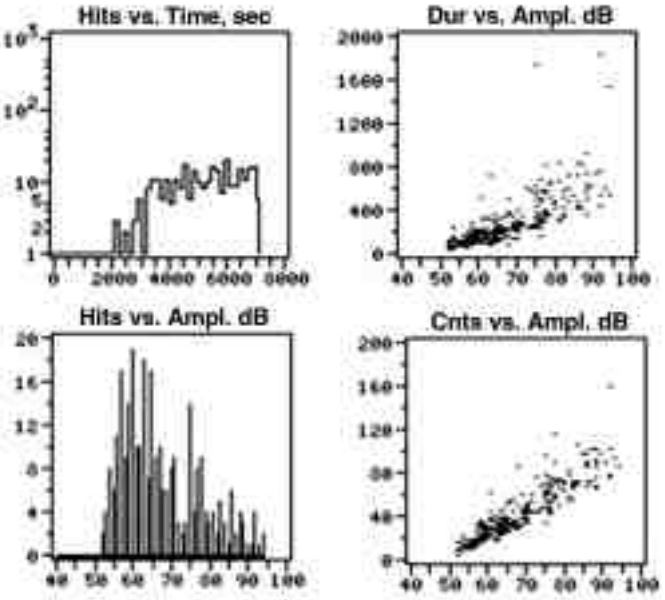

Fig. 12—SEM images of Ni-P alloy film in the end region (Solution temperature = 50°C/122°F; pH 3.5; CD = 3.0 A/dm²/27.9 A/ft²)

detection by using suitable filter and threshold settings. No crack-related AE was detected in crack-free plating. Cracks in coatings can be monitored during plating as high amplitude AE is generated. Various effects of plating conditions can be determined with AE, which can be utilized for process control during plating. However, quantitative correlation of AE and crack density requires further work as below-threshold AE signals will have to be included. Post-plating cracking behavior is also clearly indicated and can present a new research opportunity in finding cracking mechanisms.

Acknowledgment

We are grateful for the assistance of Prof. H. D. Kaesz, Dr. A. D. Bacher and Mr. C. E. Arcos of Chemistry Department of UCLA. This research was supported by a grant from the Institute for Small Business Management and Technology, Japan.

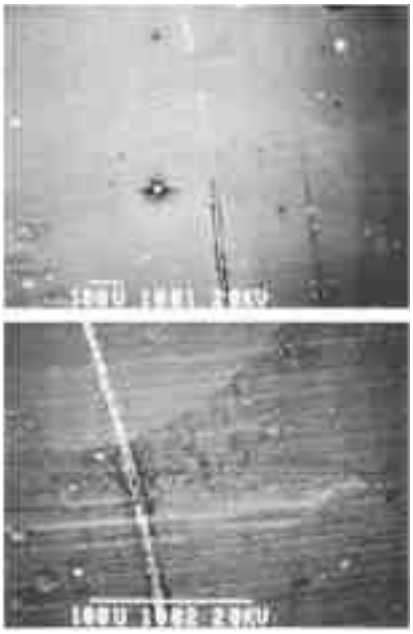

Fig. 13—Summary of AE characteristics in Ni-P plating (Solution temperature = 50°C/122°F; pH 3.5; CD = 3.0 A/dm² / 27.9 A/ft²; AE Filter = 200-1200 kHz; 56 dB threshold.)

References

1. O. Takano & K. Ono, *Proc. 2nd Int'l. Acoustic Emission Symposium*, Japanese Society for Non-Destructive Inspection, Tokyo, 1974; p. 31.
2. *Metals Handbook, 9th edition, Vol. 17: Nondestructive Testing and Quality Control*, ASM International, Materials Park, OH, 1989, p. 278.
3. *Nondestructive Testing Handbook, 2nd ed., Vol. 5: Acoustic Emission Testing*, American Society for Nondestructive Testing, Columbus, OH, 1987.
4. T.W. Rettig, & M.J. Felson, *Proc. Corrosion '74, International Corrosion Forum, Paper No.65,* NACE International, Houston, TX, 1974.

About the Authors

Dr. Tsutomu Morikawa is a Senior Staff Research Worker in the Evaluation Technology Division, Technology Res-earch Institute of Osaka Prefecture, 2-7-1, Ayumino, Izumi, Osaka, Japan. He holds a PhD degrees in engineering from University of Osaka Prefecture. His research interests includes the electroplating process for making hard coatings or amorphous films, surface analysis, material corrosion and prevention for the electroplating films.

Dr. Kanji Ono is a professor in the Department of Materials Science and Engineering, University of California, Los Angeles, California. He holds a PhD from Northwestern University. He is editor of the Journal of Acoustic Emission. *His research is about the mechanical behavior and non-destructive evaluation of structural materials.*